Bulgarian Journal of Veterinary Medicine, 2026, **29**, No 1, 20–36
ISSN 1311-1477; DOI: 10.15547/bjvm.2025-0009

Original article

IDENTIFICATION, CHARACTERISATION, AND GENE EXPRESSION ANALYSIS OF GFAP IN THE BRAIN OF RED-BELLIED PACU, *PIARACTUS ORINOQUENSIS*

J. E. LOPEZ-MURILLO[1], A. T. REYES-MUÑOZ[1], G. HOLGUIN-CÉSPEDES[1], Á. E. CÉSPEDES-RUBIO[1] & I. S. RONDÓN-BARRAGÁN[1,2]

[1]Research Group of Neurodegenerative Diseases – END, Immunotoxicology; [2]Research Group of Immunobiology and Pathogenesis; Department of Animal Health, Faculty of Veterinary Medicine and Zootechnics, University of Tolima, Ibagué, Tolima, Colombia

Summary

Lopez-Murillo, J. E., A. T. Reyes-Muñoz, G. Holguin-Céspedes, Á. E. Céspedes-Rubio & I. S. Rondón-Barragán, 2026. Identification, characterisation, and gene expression analysis of GFAP in the brain of red-bellied pacu, *Piaractus orinoquensis. Bulg. J. Vet. Med.,* **29**, No 1, 20–36.

Glial fibrillary acidic protein (GFAP) is considered a signature marker for astrocytes in several species, due to its role in cell integrity and signalling. This study aimed at the molecular characterisation of GFAP cDNA from *Piaractus orinoquensis* and to assess the gene expression in an acute brain injury model. The nucleotide sequence of *gfap* was obtained from cDNA nanosequencing and full open reading frame was amplified and confirmed by sanger sequencing. Relative gene expression was assessed in fish tissues and in the brain under an acute injury by qPCR. Western blot analysis was performed for the detection of GFAP in the brain. GFAP from *Piaractus orinoquensis* showed conserved regions and domains and GFAP transcripts were detected in all tissues. In the acute brain injury model, there was a downregulation of *GFAP* mRNA level as well as for *HIF-1a* and *GlucoR* two hours post-injury. The study of the inflammatory response modulated by astrocytes will help to understand the regulatory mechanisms in the central nervous system and the development of a piscine bio model for human and animal neuropathology. This is the first report of the full open reading frame of red-bellied pacu GFAP cDNA.

Key words: astrocytes, brain injury, fish, gene expression, type III filaments

INTRODUCTION

Intermediate filaments are fundamental components of the cytoskeleton in neurons and astrocytes (McKeon & Benarroch, 2018). Type III intermediate filament proteins include desmin, peripherin, vimentin, and glial fibrillary acid protein (GFAP) (Hol & Capetanaki, 2017). GFAP is expressed in astrocytes and other glial cells, and is considered a signature marker for astrocytes in several species (Kálmán

et al., 2013; Zhan *et al.*, 2020). It is responsible for the mechanical integrity of astrocytes and their supporting functions including cell signalling to neurons and maintenance of blood-brain barrier (McKeon & Benarroch, 2018). GFAP interacts with other proteins including intermediate filaments such as vimentin, adhesion molecules, and intracellular chaperones (McKeon & Benarroch, 2018), and it participates in mitosis by regulating filament assembly required for cytokinesis (Guichet *et al.*, 2016).

Due to its role in the pathophysiology of several neurologic disorders, including Alexander disease and neoplasia (Zhou *et al.*, 2019; Ahmadipour *et al.*, 2020), GFAP has been used as a biomarker for astrogliosis or reactive astrocytes, including in the traumatic brain injury, where it can be used for assessing severity and progression of damage and predicting patient outcomes (Lei *et al*., 2015; Li *et al.*, 2019; Brenner & Messing, 2021; Abedzadeh-Kalahroudi *et al*., 2023). Recently, GFAP quantification has been proposed as a valuable tool for the early diagnosis and monitoring of neurological disorders (Luijerink *et al*., 2024).

Fish models are used in biomedical research for studying human diseases and developing therapeutic strategies due to their physiological similarities to humans, genetic manipulation possibilities, and cost-effectiveness (Baek *et al.*, 2022). Piscine models as zebrafish have been used in neuropathological research and screening of drug candidates for neurological disorders with promising results (Probst *et al.,* 2020). In South America, including Colombia, several native fish species have been studied. The red-bellied pacu (*Piaractus orinoquensis*), a native Colombian fish, is used as a biological model in immunotoxicological and pharmacological research (Zapata-Guerra *et al.*, 2020). Recently, some neurological biomarkers have been reported in this species making it a candidate for neuropathology studies (Holguín-Céspedes *et al*., 2022; Carrillo-Godoy & Rondón-Barragán, 2023; Rueda-García & Rondón-Barragán, 2024). The aim of the present study was the molecular characterisation of GFAP cDNA from red-bellied pacu (*Piaractus orinoquensis*) and assessment of gene expression in an acute brain injury model (stab wound).

MATERIALS AND METHODS

Ethical statement

All experimental procedures followed the Guidelines from the Bioethics Committee of the Central Office of Research from University of Tolima based on Law 84/1989 and the Resolution 8430/1993 and complied with the guidelines for animal care and use in research and teaching (Jenkins *et al.*, 2014).

Experimental animals

For molecular characterisation of the GFAP gene, healthy fingerlings of red-bellied pacu *Piaractus orinoquensis* (n=3), with a body weight of 2.2–2.8 g, regardless of sex (*i.e.* both sexes) coming from the same spawning were used. The fingerlings were kept in a tank with a thermostat and constantly aerated freshwater and without a filter at a temperature of 20±1 °C and a biomass density < 1 g/L, fed twice a day a commercial diet (Solla Mojarra 30%) equivalent to 2% of the total biomass. Animals were acclimated for 21 days and treated with NaCl (1%) to prevent possible parasitic diseases. Fish were euthanised by cervical dislocation after anaesthesia by individual immersion

in a glass tank with dissolved clove oil, Eugenol 50 mg/L (Proquident S.A., Colombia) (Zapata-Guerra *et al.*, 2020). Tissue samples of brain, muscle, gut, liver, stomach, spleen, gill, blood, kidney, and heart were taken and snap-frozen in liquid nitrogen until their use.

gfap cDNA sequencing

Nucleotide *gfap* sequence was obtained from cDNA nanosequencing using the MinION sequencer (Oxford Nanopore Technologies, UK) of the brain of red-bellied pacu which was mapped on *Pygocentrus nattereri* (XM_017697492.2) and *Colossoma macropomum* (XM_036589 799.1) *gfap* gene sequences as reference templates. Primers were designed from the assembled/mapped sequence using Geneious Prime software v2025.1.2 (Biomatters Ltd, USA) (Table 1) to amplify the full open reading frame (ORF) and amplification was performed from brain cDNA of red-bellied pacu fingerlings. Before RNA extraction, tissues were thoroughly homogenised by using F6/10 handheld homogenizer (Jingxin, China). RNA was extracted by using TRIzol (Invitrogen, USA), assessed by NanoDrop™ One (Microvolume UV-Vis Spectrophotometer, ThermoFisher Scientific, USA) and cDNA was synthesised through High-Capacity cDNA Reverse Transcription kit (Thermo Fisher Scientific, USA).

Full ORF was amplified by endpoint PCR using a thermal cycler ProFlex (Applied Biosystem, USA) with volume reaction of 25 µL containing 5 µL of 5× Colorless GoTaq® Flexi Buffer, 1 µL of dNTPs mix, 1 µL of each primer (forward and reverse), 2 µL of $MgCl_2$, 0.5 U of GoTaq® Flexi DNA polymerase (Promega, Madison, USA), and 1 µL of tissue cDNA as template. PCR steps included initial denaturation at 95 °C for 3 min, followed by 35 cycles of denaturation at 95 °C for 30 s, annealing at 55 °C for 30 s, and extension at 72 °C for 1.5 min, with a final extension step at 72 °C for 7 min. Amplicons were revealed by horizontal electrophoresis using 1% agarose gel (Ultrapure™ Agarose, Thermo Fisher Scientific, USA) in a 0.5× TBE buffer. Hydragreen™ (ACT Gene, Piscataway, NJ) was used as a DNA dye and visualised under a UV gel documentation system (Enduro™ GDS, Labnet International, USA). A 100-base pair (bp) DNA ladder (New England Biolabs, USA) was included as a molecular weight marker. Amplicons were puri-

Table 1. Sequences of primers for PCR and qPCR assays

Gene	Primer sequence	Amplicon size (bp)	Accession number
*ef1a**	F- ACTGAGGTCAAGTCTGTGGA R- CCACGACGGATGTCTTTAA	110	MK085759.1
gfap ** (full ORF)	F- ATGGAGAGCCAGCGTGTCCTCTCG R- ATGGGTGAGATGTGATCAGTGC	1460	MW752483
gfap ** (qPCR)	F- GCAGGAACAGTTAATGGCTCAG R- GCCTCATACTGCACTCTGATCT	99	
HIF-1a *	F- CTACCTGCGCATGAGAAAACTTC R- ACCATGTCTCCATCCTCAGAAAGC	135	MK085762.1
GlucoR *	F- ATGAAGGTCCTGTTGCTGCTCA R- GTAGAATCGTTGCCAGTTCTGG	153	MK085760.1

Reference: * Zapata-Guerra *et al.* (2020); ** This study.

fied and sequenced by Sanger method (Macrogen Inc, Korea).

Sequence analysis, phylogenetic tree, and model structure building

Nucleotide and deduced amino acids (aa) sequence were analysed using Geneious Prime software v2025.1.2 (Biomatters Ltd, USA). Multiple sequence alignments of the peptides were generated using Geneious Prime software v2025.1.2 (Biomatters Ltd, USA), domains were predicted using InterproScan (https://www.ebi.ac.uk/interpro/search/sequence/) and conserved domains tool (https://www.ncbi.nlm.nih.gov/Structure/cdd/wrpsb.cgi). Signal peptide (http://www.cbs.dtu.dk/services/SignalP/), phosphorylation (http://www.cbs.dtu.dk/services/NetPhos/) N-linked (http://www.cbs.dtu.dk./services/NetNGlyc/) and O-linked glycosylation (http://www.cbs.dtu.dk./services/NetOGlyc/) sites were predicted using online prediction servers. A phylogenetic tree was built using the Neighbour-Joining method with 1000 bootstrap on Geneious Prime software v2025.1.2 (Biomatters Ltd, USA). The structural model of red-bellied pacu GFAP coil 1B was constructed using SWISS-MODEL (Biozentrum, Switzerland), and human GFAP (PDB accession number: 6a9p.1.A) as a template; and tender the figure with the molecular graphics system PyMOL for MacOS (Schrödinger, Inc, USA).

Western blotting of GFAP from brain tissue

Western blot analysis was performed based on Céspedes-Rubio *et al.* (2010). Briefly, the brain (telencephalon) was thawed and immediately homogenised with lysis buffer containing 150 mM NaCl, 20 mM Tris, pH 7.4, 10% glycerol, 1 mM EDTA, 1% NP40, 100 μM phenylmethylsulfonyl fluoride, 1 μg/mL aprotinin, and leupeptin (Sigma), and 100 μM orthovanadate. The sample was centrifuged at 4 °C and 1,500 rpm. The supernatant was obtained, and protein quantification was done by the modified Bradford method, using calibration standards starting from 50 mg/mL of bovine serum albumin (BSA) in deionised water and decreasing order to absolute blank. Sodium dodecyl sulfate-polyacrylamide gel electrophoresis (8-10% SDS-PAGE) was carried out using a mini-protean system (Bio-Rad, Hercules, CA) with low-range molecular weight standards (Bio-Rad). Protein (320 μg) was loaded in each lane with loading buffer containing 0.375 M Tris, pH 6.8, 50% glycerol, 10% SDS, 0.5M DTT, and 0.002% bromophenol blue. Samples were heated at 100 °C for 5 min before gel loading. After electrophoresis, proteins were transferred to nitrocellulose membranes (Amersham) using an electrophoretic transfer system (Mini-Trans-Blot Electrophoretic Transfer Cell) at 300 mA for 2 h. The membranes were washed with TTBS (20 mM Tris-HCl, pH 7.5, 500 mM NaCl, 0.05% Tween-20 containing Tris-buffered saline solution, pH 7.4) and 3% of BSA for 60 min to block nonspecific proteins epitope sites. TTBS was used for all successive washings and incubations. The membranes into selling bags were incubated for 48 hours at 4 °C with the following primary antibodies: anti-GFAP rabbit polyclonal antibody (Sigma-Aldrich, St. Louis MO., USA; reference SAB5700611 No. 2507; diluted 1:500), and anti-β-actin (ACTB) mouse AC-15 hybridoma monoclonal antibody (Sigma-Aldrich; reference No. A5441; diluted 1:2000). Membranes were washed and incubated with secondary antibodies (peroxidase-conjugated anti-rabbit IgG2 or anti-mouse IgG1; Jackson Immuno-

research Laboratories, West Grove, PA; diluted 1: 2,500) for 1 h at room temperature. The immunoreactive signal was developed by chemiluminescence ECL Western blotting system (Thermo Scientific, Rockford, IL; product No. 34080) followed by exposure of the membranes to digitalised images capture in a dark chamber at 30, 60, and 90 seconds, of exposition time in diaphragm opened remote trigged. Digital photos were analysed in Fiji Image-J software, version 1.53. ij.jar (NIH, USA). Previously, each image was processed in fotoram.io photo editor and Pixlr-E free advanced photo editor.

Gene transcripts expression in an acute brain injury model

Red-bellied pacu juveniles were used for an acute brain injury experiment following the stab wound model (Schmidt *et al.*, 2014). Six animals were kept in glass tanks with the same conditions described above and randomly distributed in two experimental groups: the control group (n=3) and the brain injury group (n=3). All individuals were anesthetised using Eugenol 50 mg/L (Proquident S.A., Colombia) (Zapata-Guerra *et al.*, 2020) for handling and any procedure. Fishes of the brain injury group were stabbed in the frontal region of the brain using a 000-gauge sterile entomological needle, with a 5 mm puncture depth performed on the left side of the skull, to reach the telencephalon and the optic lobe. All animals from the control group and brain injury group recovered from anaesthesia in a glass tank without eugenol. Two hours after stabbing, fish brain injury group were euthanised with cold water (Ferreira *et al.*, 2022) and brain samples (telencephalon and optic lobe) were taken from the left hemisphere (ipsilateral to the injury) and the right hemisphere (contralateral to the injury). The same procedure was carried out with animals from the control group. RNA extraction and cDNA synthesis were performed as described above.

RT-PCR and quantitative real-time PCR (qPCR)

RT-PCR (reverse transcription polymerase chain reaction) was conducted using qPCR primers designed based on nucleotide sequence (Table 1) to amplify a fragment of *gfap* and previously reported for *HIF-1α* and *GlucoR* genes (Zapata-Guerra *et al.*, 2020) from cDNA of the different tissues and ipsilateral and contralateral samples of the brain injury group. RT-PCR was run using a thermal cycler Proflex and GoTaq® Flexi DNA polymerase (Promega, Madison, USA), as described previously.

gfap, *GlucoR,* and *HIF-1α transcripts expression by qPCR.* Each primer product was validated by melt-curve analysis and gel electrophoresis imaging to ensure amplification from genomic DNA was not present and the specificity of the primer sequence. qPCR assays were performed using a real-time thermocycler QuantStudio™ 3 (ThermoFisher Scientific, USA) using Luna® Universal qPCR master mix (New England Biolabs, USA). Relative gene expression was calculated by $2^{-\Delta\Delta Ct}$ method (Rao *et al.*, 2013), and *ef1a* was set as a normalisation gene. Data are expressed as fold change.

Statistical analysis

Data were analysed by descriptive statistics, differences in relative gene expression in tissues of the acute injury experiment were assessed by the Student *t*-test. Statistical analyses were done with GraphPad Prism v. 10.0 for MacOS (La

Jolla, CA, USA). Differences were considered statistically significant when $P<0.05$.

RESULTS

gfap ORF contains 1338 bp that encodes for a protein of 445 aa with a molecular weight of 51218.46 Da and a theoretical pI of 5.46. Predicted peptide showed the intermediate filament head, DNA-binding domain (position 7–80), intermediate filament-rod domain (position 81–390), intermediate filament coiled coil region (position 81–117, 306–390), intermediate filament rod domain coil 1b (position 129–227), linker 1 (position 118–128), linker 1-2 (position 228–243), linker 2 (position 266–269), coil 1a (position 86–117), coil 2a (position 244–265), coil 2b (position 270–390) and a tail domain (position 391–445) (Fig. 1A).

Multiple alignment analysis demonstrated a highly conserved domains among species, with DNA-binding domain showing lower identity. Amino acid identity was high with red-bellied piranha (95.056%), and tambaqui (94.382%), and with a lower value with humans (62.247%). The signal peptide was not detected on the protein sequence and thereby *N*-glycosylations were absent. *O*-glycosylations were detected on amino acid residues 9, 19, 20, 22, 26, 27, 30, 31, 35, 38, 39, 44, 46, 47, 52–54, 57, 66, 240, 331, 334, 379, 388, 391, 396, 405, 406, 409 and 412. In addition, 25 phosphorylation sites were predicted (Fig. 1B).

The phylogenetic analysis showed that red-bellied pacu GFAP clusters with red-bellied piranha and both shared a cluster with tambaqui. In the same way, they shared a common cluster with Mexican tetra (Fig. 2).

Protein modelling was based on human GFAP Coil 1b domain (PDB accession number: 6a9p.1.A) and it showed as a homotetrameric structure comprising two equivalent parallel coiled-coil dimers that pack together in an antiparallel manner (Fig. 3B). Pairwise alignment of PoGFAP and human GFAP showed some differences in the residues (Fig. 3A), however, the intermolecular hydrogen bonds (Y116- Q117, Fig. 3B1; K134-K134, Fig. 3b2; E158-T159, Fig. 3B3; F172-R173, Fig. 3B3) and the salt bridge interactions (R141-E140, Fig. 3B2; and E158-R162, Fig. 3B3) are conserved. As described for human GFAP (Kim *et al.*, 2018), R183 (Fig. 3B5) may form a water-mediated hydrogen bond with the backbone carbonyl oxygen of E178, which allows the coiled-coil interface to complete the network. At the residue H204, each histidine has a positively charged imidazole functional group which may contribute to maintaining the coiled-coil geometry.

Multiple alignments were performed comparing GFAP amino acid sequence between red-bellied pacu, zebrafish and humans, to indicate the putative site of mutations that have been related to Alexander disease in humans. Human codons R79, R88, R258 and R416 are conserved in red-bellied pacu (R92, R101, R271 and R429) (Fig. 4). In humans GFAP, E362, and E373 correspond to R384 and R386 for red-bellied pacu. Tyrosine codon 242 in human GFAP is conserved in the red-bellied pacu but changes for phenylalanine in zebrafish.

By western blot analysis, GFAP from red-bellied pacu brain lysates showed a calculated molecular weight of 46 kDa (Fig. 5).

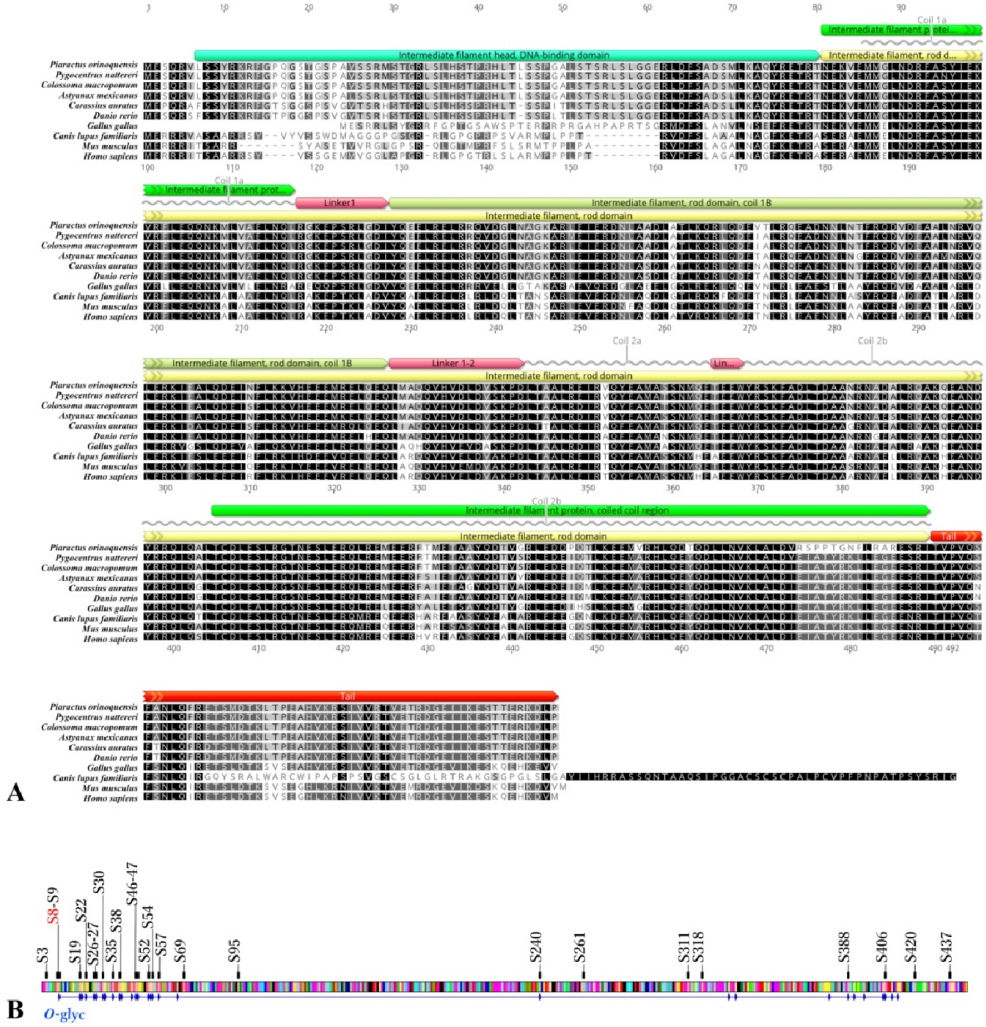

Fig. 1. Sequence analysis of GFAP from red-bellied pacu. **A.** Multiple alignment of GFAP amino acid sequences among species. Species and accession numbers are given in the supplementary file at https://trakia-uni.bg/wp-content/uploads/2025/05/Supplementary-file-2025-0009.pdf. **B.** Predicted sites of serine phosphorylation and O-glycosylation of red-bellied pacu GFAP. Phosphorylation of Ser-8 (S8) appears in red which is highly conserved among species. Glycosylation sites appear as a blue line with ticks. Phosphorylation was predicted by using NetPhos 3.1.

gfap transcript gene expression

By RT-PCR, *gfap* mRNA was detected in all tissues with an apparent lower expression in gills, blood and muscle (Fig. 6). In the brain injury model, ipsilateral *gfap*, *GlucoR* and *HIF-1α* mRNA levels were lower in animals with brain injury ($P<0.05$, $P<0.001$, $P<0.05$, respectively) compared with control group (Fig. 7A).

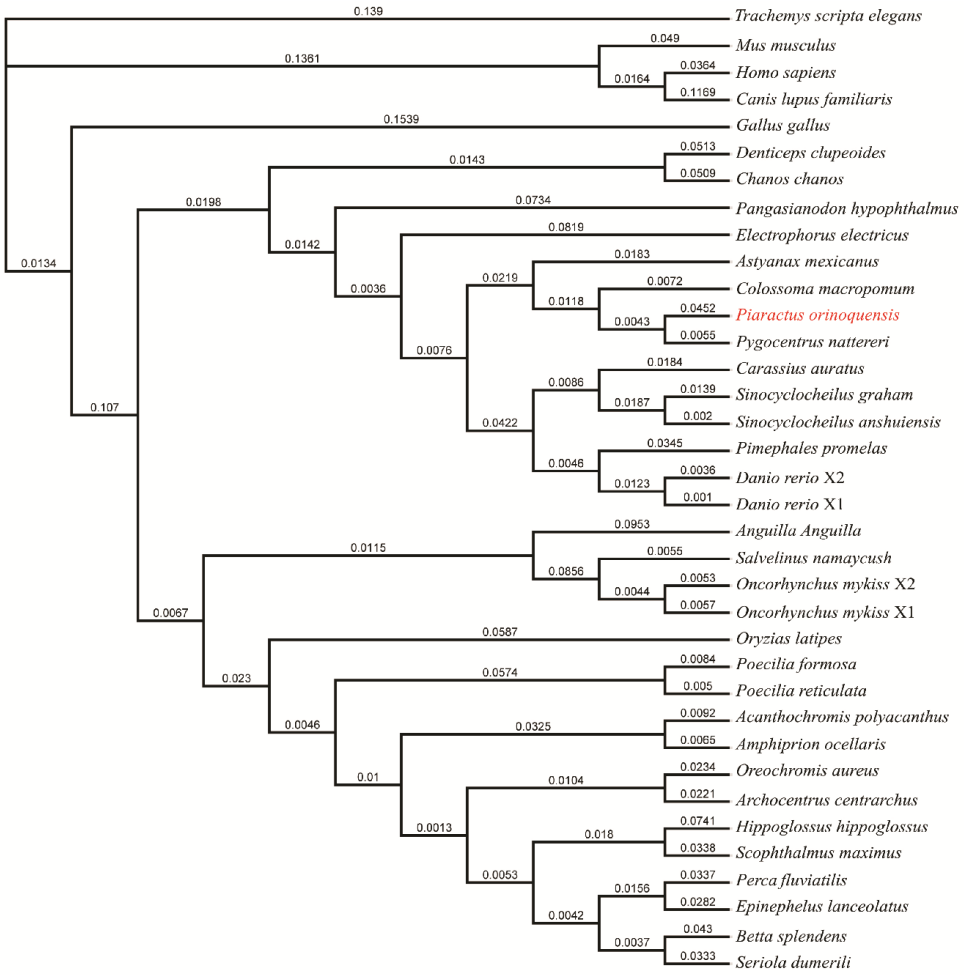

Fig. 2. Phylogenetic tree of GFAP sequences among species. Red-bellied pacu GFAP cluster with red-bellied piranha and both shared a cluster with tambaqui. Phylogenetic tree was built using N-J method with 1000 bootstrap. Branch labels represent substitutions per site. Species and accession numbers are given in the supplementary file at https://trakia-uni.bg/wp-content/uploads/2025/05/Supplementary-file-2025-0009.pdf.

Comparison of ipsilateral vs contralateral mRNA level of *gfap* showed no differences in the control group and a lower expression of *gfap* in the ipsilateral brain ($P<0.001$) compared with the contralateral brain of the injury group (Fig. 7B).

DISCUSSION

GFAP is considered a marker for differentiated astrocytes in the nervous system, but it is also expressed in foetal and adult neural stem cells in mammals (Hol & Ca-

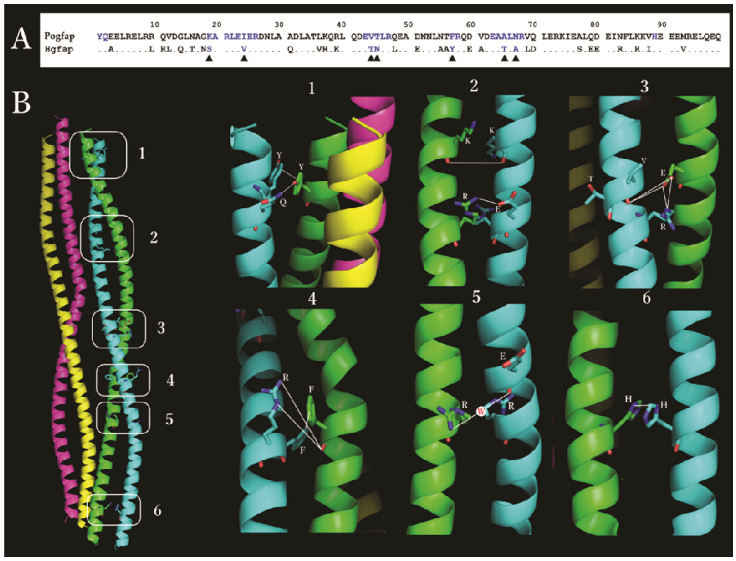

Fig. 3. Modelling of Coil 1b domain of red-bellied pacu GFAP. **A.** Pairwise alignment of red-bellied pacu GFAP Coil 1b domain and human GFAP Coil 1b domain. Blue letters correspond to the residues involved in "knobs-into-holes interactions", differences in amino acids are indicated by arrowheads below the sequence. **B.** Cartoon model of the homotetrameric red-bellied pacu GFAP Coil 1b domain. The build was done based on human GFAP (PDB accession number: 6a9p.1.A) and the interaction between amino acids were based on Kim *et al.* (2018).

```
Pogfap  MESQRVLSSYRKRFGPQGSTGSPAVSSRMSTGRLSLHSTPRHLTLSSPGALSTSRLSLGGERLDFSADSMLKAQYRETRTNEKVEMMGL  89
zgfap   .....SF........TP.GSP.VG.T..H.........S.....-...LT...................L...................  88
hgfap   ..RR.IT.AA.RSYVSS.EMMVGGLAPGRRL.PGTRL.LA.M------.PP.P.---------.V...LAGA.N.GFK...AS.RA...E.  76

Pogfap  NDRFASYIEKVRFLEQQNKMLVAELNQLRGKEPSRLGDIYQEELRELRRQVDGLNAGKARLEIERDNLAADLATLKQRLQDEVTLRQEA  178
zgfap   ..........................................................S..G.........TA.....  177
hgfap   ...................A.A.......A...TK.A.V..A......LRL.Q.T.NS....V......Q....VR.K....TN..L..  165

Pogfap  DNNLNTFRQDVDEAALNRVQLERKIEALQDEINFLKKVHEEEMRELQEQLMAQQVHVDLDVSKPDLTAALREIRVQYEAMASSNMQETE  267
zgfap   E.....................................................H.....................K...A.F....N.......  266
hgfap   E...AAY..EA...T.A.LD......S.EE..R..R.I....V.......AR.....E...A........K...T..........H.A.  254

Pogfap  EWYRSKFADLTDAANRNADALRQAKQEANDYRRQIQALTCDLESLRGTNESLERQLREMEERFTMETAAYQDTVGRLEDDPQTLKEEMV  356
zgfap   ..................GE.................G..........S..............AI.........A....EI.M.....A  355
hgfap   ..............A...EL.....H........L.S.....................M..Q...HVR.A.S..EALA...EEG.S..D..A  343

Pogfap  RHLQDTQDLLNVKLALDVRSPPTGNFLRARESRITVPVQSFANLQFRETSMDTKLTPEAHVKRSIVVRTVETRDGEIIKESTTERKDLP  445
zgfap   ....EY...........IEIATYRKL.EGE.........N.T.....D.....................................  444
hgfap   ....EY...........IEIATYRKL.EGE.N...I...T.S...I....L...SVS.G.L..N...K...M....V....KQ.H..VM  432
```

Fig. 4. Multiple alignment of amino acid sequences of red-bellied pacu GFAP (Pogfap), zebrafish GFAP (zgfap) and human GFAP (hgfap). Dots (.) indicate conserved residues, dashes (-) indicate gaps. Arrowheads indicate the position of Alexander disease mutations. Accession numbers are XP_005164040.1 for the zebrafish GFAP sequence and NP_002046.1 for human GFAP sequence.

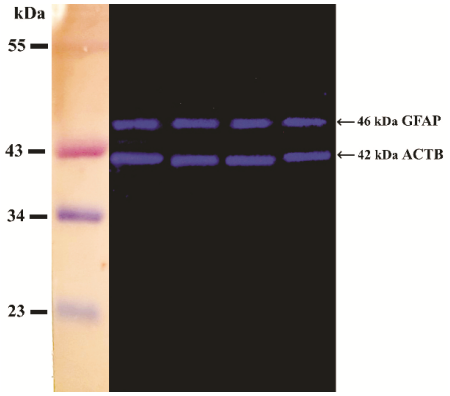

Fig. 5. Western blot detection of GFAP and ACTB from red-bellied pacu telencephalon. A band of ~46 kDa was detected using anti-GFAP antibody. A 42 kDa band corresponding to ACTB was detected.

petanaki, 2017). GFAP can be divided into three major domains: the N- terminal head region, an alpha-helical rod domain and the C-terminal tail region (Boyd *et al.*, 2012). GFAP in red-bellied pacu (PoGFAP) lacks a signal peptide and showed several O-glycosylation sites. In studies by Korolainen *et al.* (2005) O-glycosylated GFAP was common in less acidic isoforms and did not show differences between control patients and patients with Alzheimer's disease. Moreover, in PoGFAP, 25 phosphorylation sites were detected, including Ser-8, which is implicated in the regulation of filament assembly or response to injury (Sullivan *et al.*, 2012), and Ser-13, related to Alexander disease (Battaglia *et al.*, 2019). Thr-7 phosphorylation site was absent in PoGFAP since Thr7Leu occurs in this fish species. Ser-19, Ser-35, and the Ser-38 were identified in PoGFAP and they are close to phosphorylation sites Ser-17 and Ser-34/38 in hGFAP. Furthermore, Ser-388 site was detected in PoGFAP which is close to Ser-389 described in mammalian GFAP, and this phosphorylation affects interactions between intermediate filaments (proteins) and GFAP (Inagaki *et al.*, 1994). In addition, PoGFAP has a predicted molecular weight of 51.2 kDa as reported from fish and other species (Zhang *et al.*, 2014). Nevertheless, by western blot, PoGFAP showed as a band of ~46 kDa, which also has been reported as lower molecular band maybe of breakdown products of GFAP from post-mortem brain lysates as protein source (Heaven *et al.*, 2019; Zhang *et al.*, 2014).

In the Alexander disease, an autosomal dominant neurological disorder, mutations

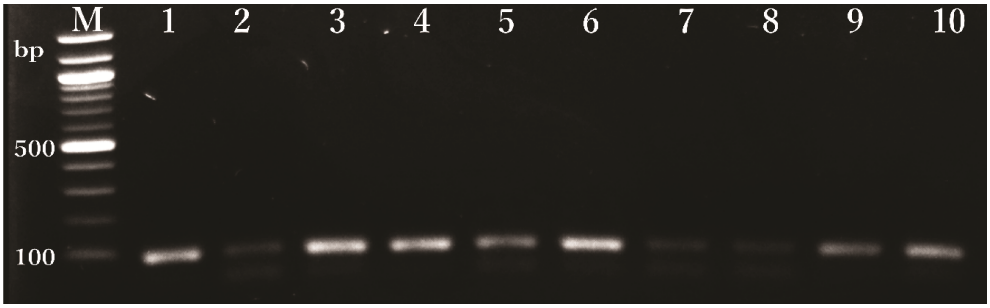

Fig. 6. Tissue expression of *gfap* transcript by RT-PCR. qPCR primers were used to amplify a 99 bp amplicon. The figure shows a representative sample (1 out of 3) for 1. Brain, 2. Muscle, 3. Gut, 4. Liver, 5. Stomach, 6. Spleen, 7. Gill, 8. Blood, 9. Kidney, 10. Heart. M. Molecular weight marker (100 bp DNA ladder, NEB).

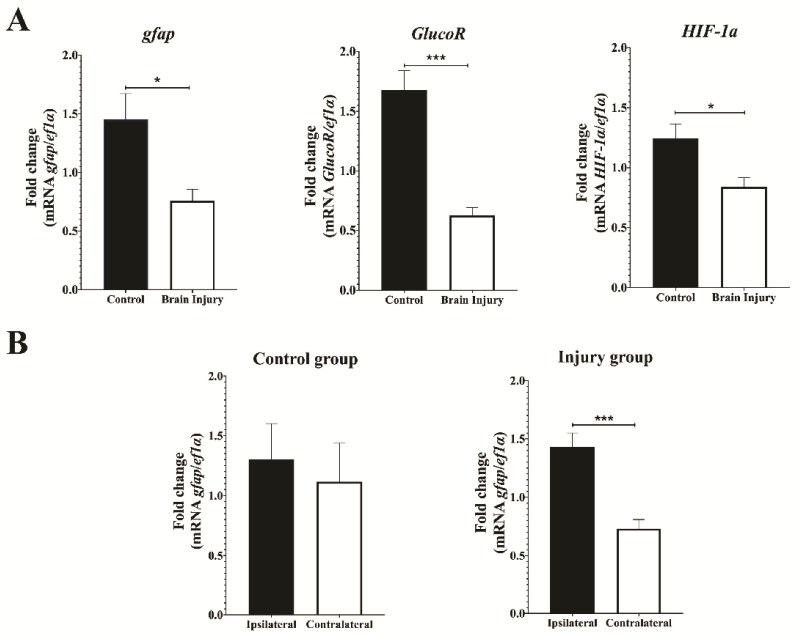

Fig. 7. Gene expression of *gfap*, *GlucoR* and *HIF-1α* transcripts in a brain injury model of red-bellied pacu. **A.** Ipsilateral expression of *gfap*, *GlucoR* and *HIF-1α* transcripts in control and brain injury group; **B.** Ipsilateral vs. contralateral expression of *gfap* transcript in control and brain injury group; *P<0.05, ***p<0.001.

of *gfap* gene resulted in elevated GFAP expression, indicating gain-of-function mutation (Ciammola *et al.*, 2019). GFAP from red-bellied pacu shares 62.2% of identity with human GFAP which is slightly lower than zebrafish with 67% (Nielsen *et al.*, 2003), however, several mutated amino acids (*n*=11) in Alexander disease are conserved among sequences. Particularly, Y242 in human GFAP is conserved in PoGFAP but is absent in zebrafish GFAP. In Alexander disease, the Y242D mutation resulted in a highly insoluble protein with abnormal circular filament organization. This tyrosine residue (Y242) in human and red-bellied pacu (Y255), as well as phenylalanine (F254) in zebrafish, are chemically distinct from the aspartic acid residue observed in Alexander disease. On the other hand, arginine at codon 239 is also conserved in PoGFAP codon 252, same as reported by Kim *et al.* (2018) for zebrafish.

In the present study, GFAP mRNA was detected in all tissues, with low expression in gills, blood, and muscle. Although GFAP is mainly expressed in astrocytes in the central nervous system, it also can be expressed by mature glial cells in the gut (Hagström & Olsson, 2010), by Schwann cells in the peripheral nervous system, and in nonneural cells in other tissues (Hol & Capetanaki, 2017). In our study, *gfap* transcript expression was downregulated in the brain injury group compared with the control group, 2 hours after stab injury. Sirko *et al.* (2015) and Baumgart *et al.* (2012) found a decrease

in the GFAP expression immediately after injury, which agrees with our results that occurred by the 2nd hour, and the authors discarded the possibility of lower expression due to loss of cellular components since cells were detected around the injury site. Previous reports by Chernoff *et al.* (2003) demonstrated an initial loss of GFAP after injury followed by an increased level in the urodele cord. In the same way, a preliminary report of GFAP expression showed a higher level of GFAP in red-bellied pacu under a chronic sublethal exposure (25 days) to chlorpyrifos and trichlorfon, together with reactive astrocytes (Reyes *et al.*, 2019). In contrast with our findings, Condorelli *et al.*, (1990) found upregulation of GFAP in the cortical zone as early as 6 h with a peak at 1–3 days in a murine brain injury model.

Furthermore, GFAP decreasing in astrocytes is linked to a loss of differentiation from cancerous cells to a blastic, less mature, more aggressive state (Hlobilkova *et al.*, 2007). Koh *et al.* (2009) showed a decrease in GFAP mRNA in U373MG cells during a relatively early stage of infection with human cytomegalovirus. In the inflammatory response in front of injury in the brain, microglia and astrocytes act as inflammatory sentinel cells in the central nervous system (Xu *et al.*, 2020), changing their morphology from a resting branched cell to a hypertrophic (ameboid) morphotype (Baumgart *et al.*, 2012), which is a less differentiated cell with high motility (Shinozaki *et al.*, 2017). The shortening of extended cytoplasmic processes is correlated with lower expression of GFAP in glioma cells (Elobeid *et al.*, 2000) which may explain the decrease in *gfap* mRNA level in our study. In the same way, Zhou & Skalli (2000) showed that low GFAP expression (mRNA) generated an increased migratory rate of glioma cells, thereby increasing the invasive potential and a low differentiation of the cells. In the inflammatory process, several surface molecules are necessary for immune cells migration through the connective tissue and blood vessels, thus the reduction in GFAP expression may be possibly related to the migratory behaviour of glial cells in the early stage of inflammation at the central nervous system in this fish species.

On the other hand, Shinozaki *et al.* (2017) showed that in a traumatic brain injury model GFAP did not change one day post-injury but was upregulated on the 3rd day at the ipsilateral side of the cortex. It may possible that at an early stage (2 h) of brain injury in our model *gfap* is downregulated and modulated by the activation of microglial cells and secretion of neuron/microglia-derived proinflammatory cytokines, *e.g.* FGF, Gal-1, Gal-3, TNF (Sirko *et al.*, 2015; Gabel *et al.*, 2016), instead of activation astrocyte population, which is considered the last glial cell type to react to injury (Robel *et al.*, 2011). In addition, in our study, there was no difference in the expression of *gfap* in the contralateral region of the brain, which is similar to the reported in traumatic brain injury model (Shinozaki *et al.*, 2017) and stab wound injury in fish (Baumgart *et al.*, 2012). This absence of contralateral response has been explained because the injury severity of the lesion does not exceed the threshold of the intensity.

Hypoxia-inducible factor 1α (HIF-1α) plays a critical role in the signalling pathway of the central nervous system injury promoting neuronal survival through regulating several gene transcripts (Gong *et al.*, 2021). In our study, brains from brain injury groups showed downregulation of *HIF-1a* 2 hours post-injury. This agrees with the findings of Shein *et al.* (2005) in

a heat acclimation experiment in the brain, where HIF-1a showed a lower expression 1 h after injury, and then the expression increase at 4 h post-injury. In the same way, in a model of ischemic brain injury, Baranova *et al.*, (2007) described that activation of HIF-1a was more relevant in the late phase (>24 h), modulating metabolic and angiogenic factors.

Glucocorticoid receptor is a member of the nuclear hormone receptor superfamily of ligand-activated transcription factors and exerts numerous functions in the brain and body and GlucoR-regulated gene networks coordinate adaptive response to stress (Timmermann *et al.*, 2019) and expression of *GlucoR* gene may change between tissues and can be regulated by several determinants including age, sex, transcription promoters, cytokines, and alarmins (Cruceanu *et al.*, 2022). In our study, *GlucoR* was downregulated in the brain injury group. This agrees with findings of Brkic *et al.* (2017) who demonstrated downregulation of the *GlucoR* in brain tissue after lipopolysaccharide treatment. Although *GlucoR* expression increases after injury, in acute response, as in our experiment, downregulation of *GlucoR* may be related to the upregulation of proinflammatory cytokines.

GFAP is highly conserved in vertebrates (Boos *et al.,* 2021), allowing piscine models in studies on neurological disorders in veterinary medicine, using it as a diagnostic biomarker improving the patient's outcome prediction. It serves as a biomarker for neuropathological conditions in horses and dogs (Loganathan *et al.,* 2024; Rohdin *et al.,* 2024). However, such studies are limited in other domestic species like swine, cattle, and cats. In conclusion, GFAP from red-bellied pacu showed conserved regions and domains like other vertebrates including humans, which makes it a candidate biomodel for neurology studies. GFAP transcripts were detected in all tissues and the acute brain injury model, at 2 h post-injury, there was a downregulation of its mRNA level as well as for *HIF-1a* and *GlucoR*. The study of the inflammatory response generated by astrocytes and their biomarkers will aid to understand the immune response in the central nervous system and the development of a piscine biomodel for human and animal neuropathology. This is the first report of the full ORF of red-bellied pacu GFAP cDNA.

ACKNOWLEDGEMENTS

This research was funded by Central Office of Research – University of Tolima, project number 310130517 "Caracterización y clonación molecular del transcripto del gen de la proteína acídica fibrilar glial (GFAP) en cachama blanca, *Piaractus orinoquensis*". The authors want to thank laboratory members, especially Julieth Michel Petano, David Rueda, and Alejandra Zapata for their help.

REFERENCES

Abedzadeh-Kalahroudi, M., E. Fakharian, M. Sehat, P. Yazdipour & M. Nejati, 2023. A study on the predictive value of glial fibrillary acidic protein for prediction of traumatic brain injury severity. *Archives of Trauma Research,* **12**, 44.

Ahmadipour, Y., O. Gembruch, D. Pierscianek, U. Sure & R. Jabbarli, 2020. Does the expression of glial fibrillary acid protein (GFAP) stain in glioblastoma tissue have a prognostic impact on survival? *Neurochirurgie,* **66**, 150–154.

Baek, K., S. Chang, C. Chang, M. Roustaei, Y. Ding, Y. Wang, J. Chen, R. O'Donnell, H. Chen, J. Ashby, X. Xu, J. Mack, S. Cavallero, M. Roper & T. Hsiai, 2022. Vascular injury in the zebrafish tail modu-

lates blood flow and peak wall shear stress to restore embryonic circular network. *Frontiers in Cardiovascular Medicine,* **9**, 841101.

Baranova, O., L. Miranda, P. Pichiule, I. Dragatsis, R. Johnson & J. Chavez, 2007. Neuron-specific inactivation of the hypoxia inducible factor 1 alpha increases brain injury in a mouse model of transient focal cerebral ischemia. *Journal of Neuroscience,* **27**, 6320–6332.

Battaglia, R., A. Beltran, S. Delic, R. Dumitru, J. Robinson, P. Kabiraj, L. Herring, V. Madden, N. Ravinder, E. Willems, R. Newman, R. Quinlan, J. Goldman, M. Perng, M. Inagaki & N. Snider, 2019. Site-specific phosphorylation and caspase cleavage of GFAP are new markers of Alexander Disease severity. *Elife,* **8**, e47789.

Baumgart, E. V., J. Barbosa, L. Bally-Cuif, M. Götz & J. Ninkovic, 2012. Stab wound injury of the zebrafish telencephalon: A model for comparative analysis of reactive gliosis. *Glia,* **60**, 343–357.

Boos, G. S., K. Failing, E. Colodel, D. Driemeier, M. de Castro, D. Bassuino, J. Diomedes Barbosa & C. Herden, 2021. Glial fibrillary acidic protein and ionized calcium-binding adapter molecule 1 immunostaining score for the central nervous system of horses with non-suppurative encephalitis and encephalopathies. *Frontiers in Veterinary Science,* **8**, 660022.

Boyd, S., B. Nair, S. Ng, J. Keith & J. Orian, 2012. Computational characterization of 39 splice variants in the GFAP isoform family. *PLoS ONE* **7**, e33565.

Brenner, M. & A. Messing, 2021. Regulation of GFAP Expression. *ASN Neuro,***13**, 1759091420981206.

Brkic, Z., E. Francija, Z. Petrovic, D. Franic, I. Lukic, M. Mitic & M. Adzic, 2017. Distinct modifications of hippocampal glucocorticoid receptor phosphorylation and FKBPs by lipopolysaccharide in depressive female and male rats. *Journal of Psychopharmacology,* **31**, 1234–1249.

Carrillo-Godoy, N. & I. Rondón-Barragán, 2023. Molecular characterization of high mobility group box 1a (HMGB1a) gene in red-bellied pacu, *Piaractus brachypomus*. *Veterinary Medicine International,* **2023**, 2774528.

Céspedes-Rubio, A., F. Jurado & G. Cardona-Gómez, 2010. p120 catenin/αN-catenin are molecular targets in the neuroprotection and neuronal plasticity mediated by atorvastatin after focal cerebral ischemia. *Journal of Neuroscience Research,* **88**, 3621–3634.

Chernoff, E. A., D. Stocum, H. Nye & J. Cameron, 2003. Urodele spinal cord regeneration and related processes. *Developmental Dynamics,* **226**, 295–307.

Ciammola, A., D. Sangalli, J. Sassone, B. Poletti, L. Carelli, P. Banfi, G. Pappacoda, I. Ceccherini, A. Grossi, L. Maderna, M. Pingue, F. Girotti & V. Silani, 2019. A novel mutation of GFAP causing adult-onset Alexander Disease. *Frontiers in Neurology,* **10**, 1124.

Condorelli, D. F., P. Dell'albani, L. Kaczmarek, G. Messina, G. Spampinato, R. Avola, A. Messina & A. Guiffrida, 1990. Glial fibrillary acidic protein messenger RNA and glutamine synthetase activity after nervous system injury. *Journal of Neuroscience Research,* **26**, 251–257.

Cruceanu, C., L. Dony, A. Krontira, D. Fischer, S. Roeh, R. Di Giaimo, C. Kyrousi, L. Kaspar, J. Arloth, D. Czamara, N. Gerstner, S. Martinelli, S. Wehner, M. Breen, M. Koedel, S. Sauer, V. Sportelli, M. Rex-Haffner, S. Cappello, F. Theis & E. Binder, 2022. Cell-type-specific impact of glucocorticoid receptor activation on the developing brain: A cerebral organoid study. *American Journal of Psychiatry,* **179**, 375–387.

Elobeid, A., E. Bongcam-Rudloff, B. Westermark & M. Nistér, 2000. Effects of inducible glial fibrillary acidic protein on glioma cell motility and proliferation. *Journal of Neuroscience Research,* **60**, 245–256.

Ferreira, J. M., L. Felix, S. Jorge, S. M. Monteiro, I. Olsson & A. Valentim, 2022. Anesthesia overdose versus rapid cooling for euthanasia of adult zebrafish. *Zebrafish,* **19**, 148–159.

Gabel, S., E. Koncina, G. Dorban, T. Heurtaux, C. Birck, E. Glaab, A. Michelucci, P. Heuschling, L. Grandbarbe, 2016. Inflammation promotes a conversion of astrocytes into neural progenitor cells via NF-κB activation. *Molecular Neurobiology,* **53**, 5041-5055.

Gong, C., L. Liu & Y. Shen, 2021. Biomarkers mining for spinal cord injury based on integrated multi-transcriptome expression profile data. *Journal of Orthopaedic Surgery and Research,* **16**, 267.

Guichet, P-O., S. Guelfi, C. Ripoll, M. Teigell, J. Sabourin, L. Bauchet, V. Rigau, B. Rothut & J. Hugnot, 2016. Asymmetric distribution of GFAP in glioma multipotent cells. *PLoS ONE* **11**, e0151274.

Hagström, C. & C. Olsson, 2010. Glial cells revealed by GFAP immunoreactivity in fish gut. *Cell Tissue and Research,* **341**, 73–81.

Heaven, M. R., L. Wilson, S. Barnes & M. Brenner, 2019. Relative stabilities of wild-type and mutant glial fibrillary acidic protein in patients with Alexander disease. *Journal of Biological Chemistry,* **294**, 15604–15612.

Hlobilkova, A., J. Ehrmann, E. Sedlakova, V. Krejci, P. Knizetova, M. Fiuraskova, M. Kala, O. Kalita & Z. Kolar, 2007. Could changes in the regulation of the PI3K/PKB/Akt signaling pathway and cell cycle be involved in astrocytic tumor pathogenesis and progression? *Neoplasma,* **54**, 334–341.

Hol, E. M. & Y. Capetanaki, 2017. Type III intermediate filaments desmin, Glial Fibrillary Acidic Protein (GFAP), vimentin, and peripherin. *Cold Spring Harbor Perspectives in Biology*, **9**, a021642.

Holguín-Céspedes, G. K., Á. E. Céspedes-Rubio & I. S. Rondón-Barragán, 2022. First study on response of astrocytes in alevines of red-bellied pacu (*Piaractus brachypomus*) to subchronic exposure to chlorpyrifos and trichlorfon. *Veterinary World,* **15**, 1676–1683.

Inagaki, M., Y. Nakamura, M. Takeda, T. Nishimura, N. Inagaki, 1994. Glial fibrillary acidic protein – dynamic property and regulation by phosphorylation. *Brain Pathology,* **4**, 239–243.

Jenkins, J. A., H. Chair, J. Bart, J. Bowker, P. Bowser, J. Macmillan, J. Nickum, J. Rose, P. Sorensen, G. Whitledge, J. Rachlin, B. Warkentine & H. Bart, 2014. Guidelines for the Use of Fishes in Research. Bethesda, Maryland, USA: American Fisheries Society.

Kálmán, M., H. Somiya, L. Lazarevic, I. Milosevic, C. Ari & K. Majorossy, 2013. Absence of post□lesion reactive gliosis in elasmobranchs and turtles and its bearing on the evolution of astroglia. *Journal of Experimental Zoology Part B, Molecular Development Evolution,* **320B**, 351–367.

Kim, B., S. Kim & M. Jin, 2018. Crystal structure of the human glial fibrillary acidic protein 1B domain. *Biochemical and Biophysical Research Communications,* **503**, 2899–2905.

Koh, K., K. Lee, J. Ahn & S. Kim, 2009. Human cytomegalovirus infection downregulates the expression of glial fibrillary acidic protein in human glioblastoma U373MG cells: Identification of viral genes and protein domains involved. *Journal of General Virology,* **90**, 954–962.

Korolainen, M. A., S. Auriola, T. Nyman, I. Alafuzoff & T. Pirttilä, 2005. Proteomic analysis of glial fibrillary acidic protein in Alzheimer's disease and aging brain. *Neurobiology of Disease,* **20**, 858–870.

Kumar, H. S., A. Wisner, J. Refsnider, C. Martyniuk & J. Zubcevic, 2023. Small fish, big discoveries: Zebrafish shed light on microbial biomarkers for neuro-immune-cardiovascular health. *Frontiers in Physiology,* **14**, 1186645.

Lei, J., G. Gao, J. Feng, Y. Jin, W. Chuanfang, Q. Mao & J. Jiang, 2015. Glial fibril-

lary acidic protein as a biomarker in severe traumatic brain injury patients: A prospective cohort study. *Critical Care,* **19**, 362.

Li, T., X. Chen, C. Zhang & Y. Wenglong, 2019. An update on reactive astrocytes in chronic pain. *Journal of Neuroinflamation,* **16**, 140.

Loganathan, N., C. Lieu & D. Belsham, 2024. Immortalization and characterization of GFAP-expressing glial cells from the adult mouse hypothalamus, cortex, and brain stem. *Neuroscience,* **551**, 43–54.

Luijerink, L., M. Rodriguez & R. Machaalani, 2024. Quantifying GFAP immunohistochemistry in the brain – introduction of the reactivity score (R-score) and how it compares to other methodologies. *Journal of Neuroscience Methods,* **402**, 110025.

Mckeon, A. & E. Benarroch, 2018. Glial fibrillary acid protein functions and involvement in disease. *Neurology*, **90**, 925-930.

Nielsen, A. L., I. Holm, M. Johansen, B. Bonven, P. Jørgensen & A. Jørgensen, 2002. A new splice variant of glial fibrillary acidic protein, GFAP epsilon, interacts with the presenilin proteins. *Journal of Biological Chemistry,* **277**, 29983–29991.

Rao, X., X. Huang, Z. Zhou & X. Lin, 2013. An improvement of the 2ˆ(-delta delta CT) method for quantitative real-time polymerase chain reaction data analysis. *Biostatistics, Bioinformatics and Biomathematics,* **3**, 71–85.

Reily, C., T. Stewart, M. Renfrow & J. Novak, 2019. Glycosylation in health and disease. *Nature Reviews Nephrology,* **15**, 346–366.

Reyes, A., J. López, G. Holguín, A. Céspedes & I. Rondón, 2019. Astrocytic response in chronic sublethal exposure to chlorpyrifos and trichlorfon on juveniles of red-bellied pacu, *Piaractus brachypomus*. *Revista Colombiana de Ciencias Pecuarias,* **32**, 152.

Robel, S., B. Berninger & M. Götz, 2011. The stem cell potential of glia: Lessons from reactive gliosis. *Nature Reviews Neuroscience*, **12**, 88–104.

Rohdin, C., I. Ljungvall, K. Jäderlund, A. Svensson, K. Lindblad-Toh & J. Häggström, 2024. Assessment of glial fibrillary acidic protein and anti-glial fibrillary acidic protein autoantibody concentrations and necrotising meningoencephalitis risk genotype in dogs with pug dog myelopathy. *The Veterinary Record* **194**, e3895.

Rueda-García, V. & I. Rondón-Barragán, 2024. Molecular characterization of neurogranin (NRGN) gene from red-bellied pacu (*Piaractus brachypomus*). *Molecular Neurobiology,* **61**, 2620–2630.

Schmidt, R., T. Beil, U. Strahle & S. Rastegar, 2014. Stab wound injury of the zebrafish adult telencephalon: A method to investigate vertebrate brain neurogenesis and regeneration. *Journal of Visual Experiments,* **90**, e51753.

Shein, N. A., M. Horowitz, A. Alexandrovich, J. Tsenter & E. Shohami, 2005. Heat acclimation increases hypoxia-inducible factor 1 alpha and erythropoietin receptor expression: Implication for neuroprotection after closed head injury in mice. *Journal of Cerebral Blood Flow & Metabolism,* **25**, 1456–1465.

Shinozaki, Y., K. Shibata, K. Yoshida, E. Shigetomi, C. Gachet, K. Ikenaka, K. Tanaka & S. Koizumi, 2017. Transformation of astrocytes to a neuroprotective phenotype by microglia via P2Y1 receptor downregulation. *Cell Reports,* **19**, 1151–1164.

Sirko, S., A. Neitz, T. Mittmann, A. Horvat-Bröcker, A. Von Holst, E. Ulf & A. Faissneret, 2009. Focal laser-lesions activate an endogenous population of neural stem/progenitor cells in the adult visual cortex. *Brain,* **132**, 2252–2264.

Sullivan, S. M., R. Sullivan, S. Miller, Z. Ireland, S. Bjorkman, D. Pow & P. Colditz, 2012. Phosphorylation of GFAP is associated with injury in the neonatal pig hypoxic-ischemic brain. *Neurochemical Research,* **37**, 2364–2378.

Timmermans, S., J. Souffriau & C. Libert, 2019. A general introduction to glucocor-

ticoid biology. *Frontiers in Immunology* **10**, 1545.

Xu, S., J. Lu, A. Shao, J. Zhang & J. Zhang, 2020. Glial cells: Role of the immune response in ischemic stroke. *Frontiers in Immunology,* **11**, 294.

Zapata-Guerra, N. A., D. Rueda-Gómez, K. Lozano-Villegas, M. Herrera-Sánchez, H. Uribe-García & I. Rondón-Barragán, 2020. Menthol as anaesthetic for red-bellied pacu (*Piaractus brachypomus*) and its effect on *HIF1a* and *GlucoR* gene expression. *Aquaculture Research,* **0**, 1–9.

Zhang, Z., J. Zoltewicz, S. Mondello, K. Newsom, Z. Yang, B. Yang, F. Kobeissy, J. Guingab, O. Glushakova, S. Robicsek, S. Heaton, A. Buki, J. Hannay, M. Gold, R. Rubenstein, X. Lu, J. Dave, K. Schmid, F. Tortella, C. Robertson & K. Wang, 2014. Human traumatic brain injury induces autoantibody response against glial fibrillary acidic protein and its breakdown products. *PLoS ONE,* **9**, e92698.

Zhou, B., Y. Zuo & R. Jiang, 2019. Astrocyte morphology: Diversity, plasticity, and role in neurological diseases. *CNS Neuroscience Therapy,* **25**, 665–673.

Zhou, R. & O. Skalli, 2000. TGF-a differentially regulates GFAP, vimentin, and nestin gene expression in U-373 MG glioblastoma cells: Correlation with cell shape and motility. *Experimental Cell Research,* **254**, 269–278.

Paper received 22.01.2025; accepted for publication 02.05.2025

Correspondence:

Iang Schroniltgen Rondón-Barragán
Department of Animal Health
Faculty of Veterinary Medicine and Zootechnics, University of Tolima
Santa Helena Highs,
730006299, Ibagué, Tolima, Colombia
e-mail: isrondon@ut.edu.co
https://orcid.org/0000-0001-6980-892X